sustainability

MDPI

Article

Compressed Earth Blocks Using Sediments and Alkali-Activated Byproducts

Fouad Belayali [1,2,*], Walid Maherzi [1,2,*], Mahfoud Benzerzour [1,2], Nor-Edine Abriak [1,2] and Ahmed Senouci [3]

[1] IMT Nord Europe, Institut Mines-Télécom, Centre for Materials and Processes, F-59000 Lille, France; mahfoud.benzerzour@imt-nord-europe.fr (M.B.); nor-edine.abriak@imt-nord-europe.fr (N.-E.A.)
[2] ULR 4515—LGCgE—Laboratoire de Génie Civil et géo-Environnement, University Lille, F-59000 Lille, France
[3] Department of Construction Management, University of Houston, Houston, TX 77204-4020, USA; asenouci@central.uh.edu
* Correspondence: fouad.balayali@imt-nord-europe.fr (F.B.); walid.maherzi@imt-lille-douai.fr (W.M.)

Abstract: Sediment dredging is necessary and vital to preserve maritime activities and prevent floods. The management of these sediments represent an environmental challenge for many countries all over the world. This study focuses on evaluating the feasibility of using dredged sediments for the manufacturing of compressed earth blocks (CEB). The alternative construction material has the potential of reducing the need for dredged sediment onshore storage or ocean dumping. Several experimental tests have been conducted on two geopolymer types, which were obtained by mixing sediments from the northern region of France, fly ash (FA), and grounded blast furnace slag (GBFS). The geopolymers, which were activated using an eight-molar concentrated sodium hydroxide solution (NH), were cured at a temperature of 50 °C. The results have shown that a geopolymer content of 36% of FA and 10% of GBFS along with (NH) alkaline solution has significantly improved the mechanical properties of CEBs, which have outperformed those of Portland Cement-stabilized traditional blocks. The use of NH has resulted in the formation of crystalline calcium silicate hydrate (C-S-H) amorphous gel. Adding GBFS to the mix has enhanced the geopolymer paste compressive strength and microstructure because of the formation of additional C-S-H. The valorization of dredged sediments in CEB based on geopolymer stabilization can contribute to the reduction of the CO_2 footprint of the construction industry.

Keywords: valorization; byproduct; compressed sediment blocks; sediment; fly ash; grounded furnace blast slag; geopolymers; circular economy; waste management

check for updates

Citation: Belayali, F.; Maherzi, W.; Benzerzour, M.; Abriak, N.-E.; Senouci, A. Compressed Earth Blocks Using Sediments and Alkali-Activated Byproducts. *Sustainability* **2022**, *14*, 3158. https://doi.org/10.3390/su14063158

Academic Editor: Antonio Caggiano

Received: 7 February 2022
Accepted: 2 March 2022
Published: 8 March 2022

1. Introduction

Today, saving natural resources and combating climate change are two major challenges faced by our planet to ensure good living conditions for mankind in the future. Natural resources, such as fossil fuels, are not renewable. The reuse and recycling of waste could save raw materials and energy and reduce greenhouse gas emissions. Indeed, Pierrehumbert et al. [1] have reported that the carbon dioxide emissions in the atmosphere through activities, such as fossil fuel burning, cement production, and deforestation, need to be reduced to zero. The lack of progress towards the reduction of carbon dioxide emissions has created justifiable panic about the world climate. The use of sediments in building materials can save natural resources and promote a disposal solution that does not disturb the ecosystem. Dredging is often necessary to restore the natural environment and the navigation required depth. In France, approximately 50 million m^3 of sediments are dredged, stored, treated, or transported abroad each year, compared to 300 million m^3 in Europe [2] and nearly 300 million m^3 in the United States.

Due to limited storage capacity, many countries have recently adopted reuse strategies for dredged materials. In the last few decades, many solutions and methodologies have been developed worldwide for the beneficial reuse of dredged materials.

Due to natural resource shortage and increased environmental regulations, the use of alternative materials in the construction industry [3], such as sediments, represents appropriate solutions for sustainable development. For several years, the main topic of global environmental policies (Kyoto Protocol (1995); COP 21 (2015)) has focused on the optimized and efficient use of by-products such as sediments.

Moreover, the reuse of alternative materials has become a solution to reduce high levels of CO_2 emissions into the atmosphere, which represent considerable financial burdens and environmental challenges. Indeed, the construction industry consumes large amounts of raw materials (about 1 million tons/day) [4,5]. Therefore, the building sector is one of the areas where an action is imperative. The sediments can potentially be used as alternative aggregates in the sector, especially in concrete, bricks etc. Dredged sediment can also be incorporated as sand in compressed earth blocks (CEB) [6], whose production consumes less energy than that of clay blocks [5].

The use of traditional binders such as Portland cement or lime for the manufacture of CEBs yield modest mechanical and physical properties (for example, compressive strength ranging between 2 and 4 MPa), including thermal. In addition, the use of cement and lime has an environmental impact because it generates significant greenhouse gas emissions [4,5]. The negative impacts of traditional block production (mechanical, physical, and economic) make finding alternative construction materials appropriate, even essential. Today, the possibility of stabilizing the earth with a geopolymer binder has become a reality to limit the production of greenhouse gases related to the manufacture of cement and to respond to habitat problems.

Geopolymer materials are mineral polymers containing activated silica (SiO_2) and alumina (Al_2O_3), such as fly ash (FA), MK750 Metakaolin, and granulated blast furnace slag (GBFS), which come into contact with alkaline solutions (activator) [7,8]. Several solutions have already been tested for sodium hydroxide and calcium hydroxide sodium silicate. Fly ash is a by-product of thermal power plants [7,9]. There are two types of fly ash, namely, high calcium and SiO_2 contents. Both types of fly ash are rich in Al_2O_3 alumina [10,11]. Silicates and alumina are two chemical elements that make fly ash a good precursor to the formulation of geopolymers. Moreover, the calcium contained in the fly ash [12,13] improves the development of the geopolymer resistance due to the additional formation of hydrated calcium silicate (CSH) [14] that coexists with the geopolymer products [15,16].

Blast furnace slag is generally used as an additive in concrete because of its high content of CaO, SiO_2, and Al_2O_3 in the amorphous state [17,18], which confers the pozzolanic properties in alkaline solutions. Several studies have examined the incorporation of GBFS into the geopolymer matrix [7,18,19]. GBFS has increased the calcium in the system and has improved mechanical properties and microstructure of geopolymers through the alkaline activation of GBFS that generates CSH and/or CASH gels [20]. On the other hand, the main alkaline activation product of FA is NASH gel. The objective of this paper is to study the physical and mechanical behavior of compressed earth blocks using the sediment in the raw state as sand and to analyze its microstructure. The results obtained are expected to be beneficial for the understanding and future applications of FA-GBFS geopolymers.

2. Materials and Methods

2.1. Materials

2.1.1. Dredged Sediments

The sediment (S) was sieved at 5 mm to obtain a granular class material of 0/5 mm while respecting the normative recommendations ARS 674 [21].

2.1.2. Binders

Fly Ash (FA) was supplied by the company SURSCHIST in Hornaing, France. On the other hand, the granulated blast furnace slag crushed (GBFS) was supplied by the company ECOCEM in Fos-sur-Mer, France. The FA and GBFS were used as precursors to produce the geopolymerisation reactions. A solution of sodium hydroxide (NH) with a molarity of 8 M, which was obtained by dissolving the crystals of NaOH with a purity of 99% in distilled water, was used as the activation solution the aluminosilicate constituting the FA and the GGBS.

2.2. Mixtrues Design

To obtain a CEB optimal packing density, the optimal density method has been adopted using the Proctor test of the sediments (S), fly ash (FA), and ground blast furnace slag (GBFS) by increasing the content of water added to the mixes [22] as illustrated in Figure 1a. The homogenization of the materials mix was carried out to ensure a good distribution of the fly ash particles in the sediment. Five water content has been considered in this test to determine the optimal water content by sweeping all possible densities (Figure 2). This allows adjustment of the quantity of the alkaline solution, which must be put for the geo-polymerization.

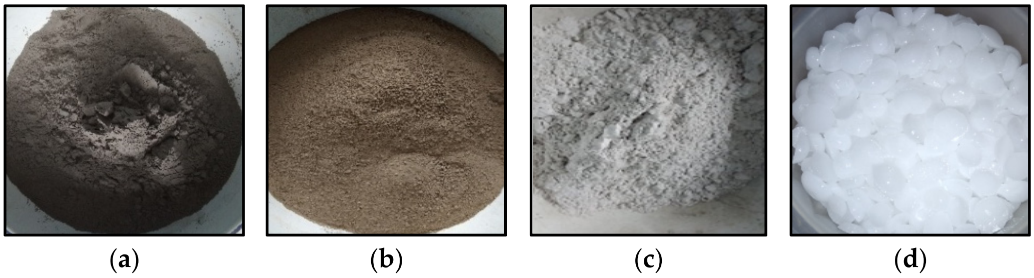

Figure 1. Compressed Block Materials. (**a**) Fly Ash class F. (**b**) Sediment 0/5 mm. (**c**) Ground Blast Furnace Slag. (**d**) Sodium Hydroxide pellet.

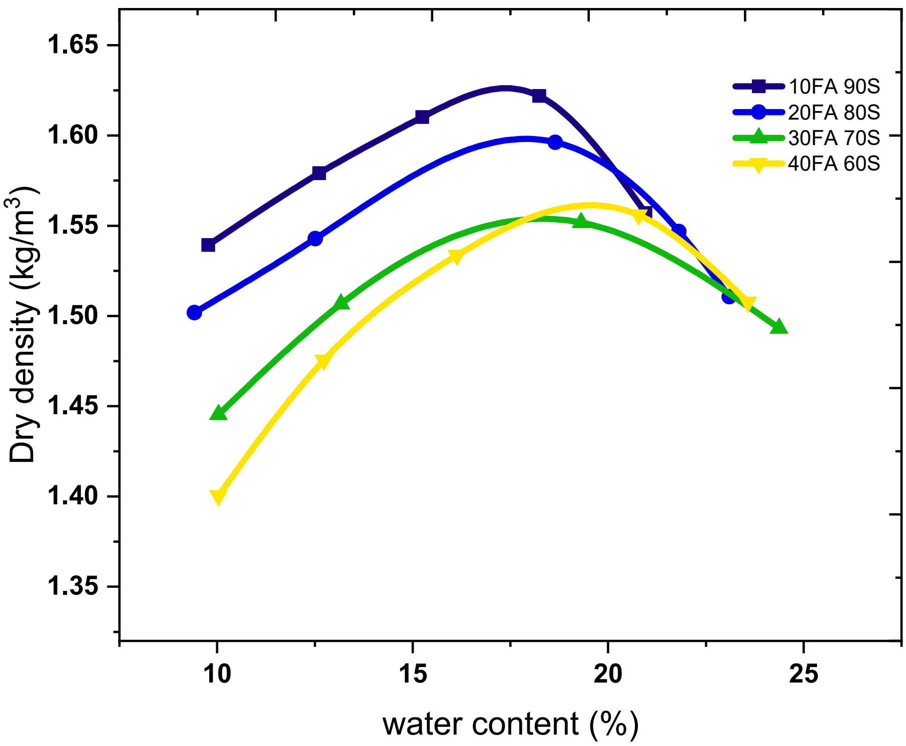

Figure 2. Mix optimum water contents (sediment fly Ash).

2.3. CEB Preparation and Hardening Conditions

The homogenization has been carried out using a Controlab mixer to sufficiently achieve a perfect mix. The test specimens chosen in this study are cylindrical-shaped plugs with 50 mm in diameter and 100 mm in height (Figure 3a). After homogenization of the dry mixtures (sediment and fly ash) for 10 min, the mixtures were moistened by adding the prepared alkaline activation solution with the corresponding water content to the optimum Proctor and the sodium hydroxide. After that, the mixtures were compacted with static compaction method at a maximal pressure of 40 bars. The static compression was performed in 3 steps. This method makes it possible to gradually obtain the final dimension of the sample according to the standard NF P 94-100 [23]. After compressing the sample, the load was kept for 10 s, and then the specimens were removed from molds using a piston, as shown in Figure 3. The formulations and compositions of the compressed blocks are shown in Table 5.

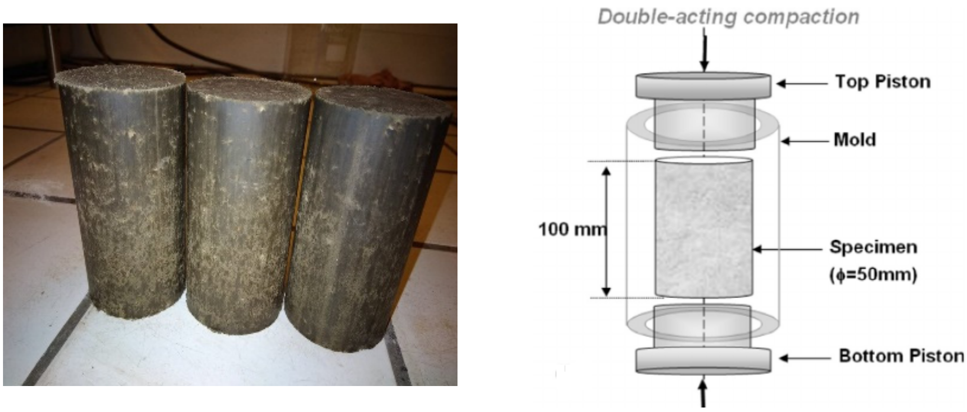

(**a**) (**b**)

Figure 3. (**a**) Sample preparation; (**b**) device and specimens.

The obtained specimens were covered with a plastic film to maintain humidity and prevent water evaporation. Furthermore, they were placed for 7 days in an oven at a temperature of 50 ± 5 °C to accelerate the geopolymer reaction. The specimens were then placed in a climatic chamber at a room temperature for 14 and 28 days before their characterization.

2.4. Analysis Methods

The sediment and the precursors (FA and GBFS) were analyzed by XRD using BRUCKER AXS D8 ADVANCE, by X-rays using energy dispersal, and SEM using JEOL electron microscope to determine their mineralogical composition and their morphology. The particle size distribution, plasticity, absolute density, specific surface, and Proctor compaction were carried out according to the standards listed in Table 1.

Table 1. Physical characterization methods.

Particle size distribution (sediment)	Grain size (X11-667 [24])
Clay fraction quantity	Methylene Blue Value—MBV (NF P94-068 [25])
Density	Helium pycnometer (NF EN 1097-7 [26])

2.5. Physical and Mechanical Characterization of CEBs

2.5.1. Water Resistance

It is essential to investigate the behavior of the compressed blocks under humid conditions, in particular rainwater [27]. The cylindrical specimens were immersed in a water container containing about 1000 mL of distilled water at room temperature for 92 h. The investigation of the behavior of the blocks in water was carried out visually through the changes in the initial color of the water. A no-color water change means a block with very good cohesion. On other hand, a yellowed water means a non-stability of the block, which may lead to a collapse later.

2.5.2. Compressive Strength

The mechanical strengths of the dry blocks were achieved using a hydraulic press (ARISTON) with a capacity of 300 KN at a loading rate of 11.78 KN/min according to NF EN 196-1 [28]. However, three samples were tested for each formulation to ensure the repeatability of the results.

2.5.3. Capillary Water Test

The capillary water absorption test, which simulates the saturation of the blocks with water in a case of severe thunderstorms, was measured according to standard XP P 13-901 [29]. The test consists of immersing the sample surface in a 5-mm thin water layer for 10 min and to visualize the mass gain of the brick during this test (Figure 4). The water absorption coefficient is derived from this test is given by the following formula:

$$\text{Cb} = \frac{100 * (P1 - P0)}{S\sqrt{t}} \left(\text{g/cm}^2\ \text{min}^{\frac{1}{2}}\right)$$

Cb: coefficient of resistance to capillary rise
$P1$: weight of the block after immersion in water (g)
$P0$: weight of the block before immersion in water (g)
S: submerged surface (cm^2)
t: water immersion time (min)

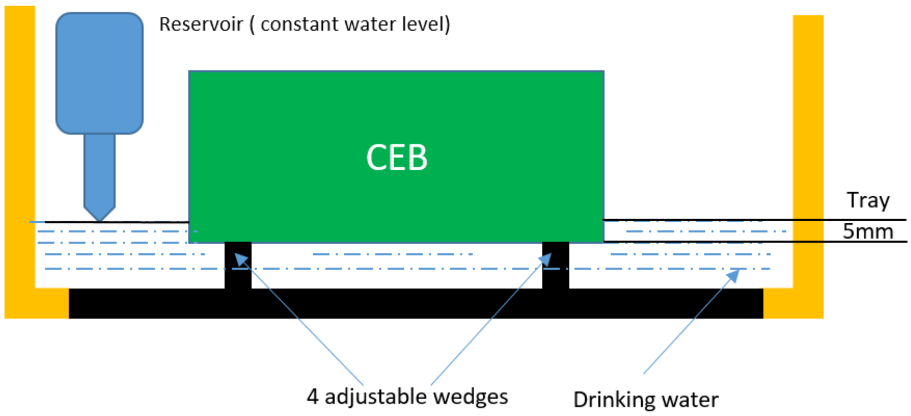

Figure 4. Capillary absorption test schema.

3. Results and Discussion

3.1. Basic Material Characterization

The materials used herein were the fluvial sediment dredged at Aire-sur-la-Lys in northern France, Fly ash (FA) from the SURSCHISTE plant, and granulated blast furnace slag (GBFS) from ECOCEM France in Fos-sur-Mer. The diffractometer shows that sediment is mainly composed of quartz, calcite, and some traces of muscovite, montmorillonite, and rutile (Figure 5A).

The DRX results of FA and GBFS are shown in Figure 5B. They indicate that FA has a predominantly amorphous mineralogical structure consisting of a bump around 18–28 _2theta with some crystalline phases such as mullite ($Al_6Si_2O_{13}$), quartz (SiO_2), magnesium ferrite (Fe_2MgO_4). On the other hand, the results show that GBFS is predominantly made up of amorphous phase, consisting of a bump around 25–35 _2-theta [19] with a small amount of magnetite.

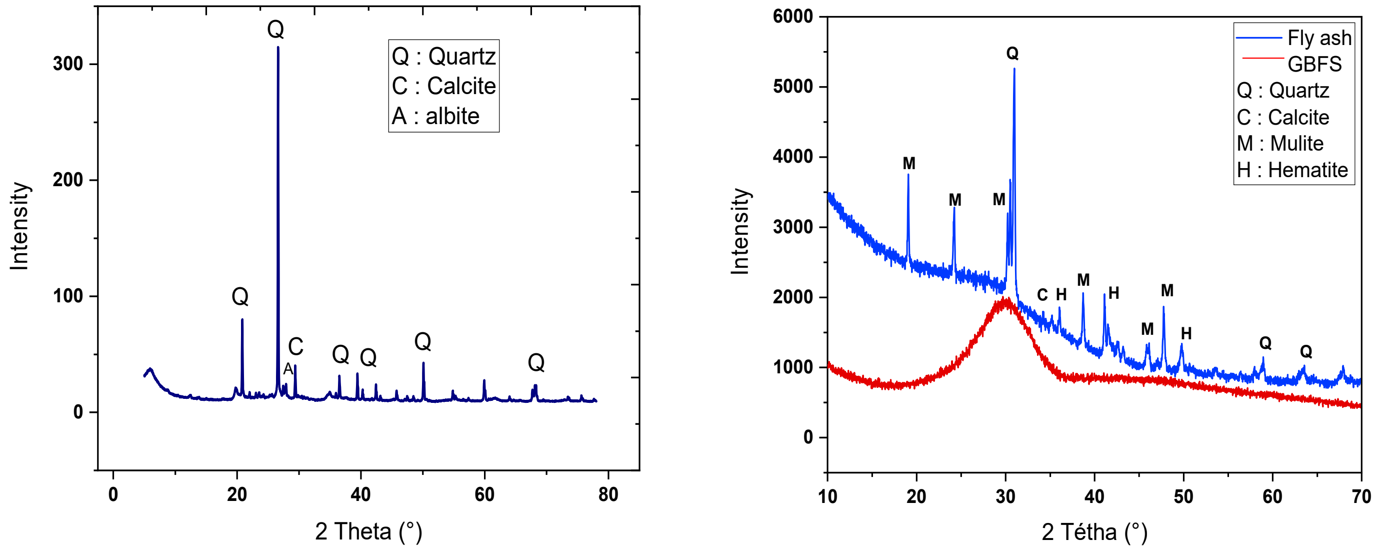

(**A**) (**B**)

Figure 5. (**A**) Raw sediment XRD; (**B**) Precursor powders (FA and GBFS) XRD.

The results of the X-ray fluorescence test allow to quantify the percentage of the material main oxides. According to the results summarized in Table 2, the sediment predominant oxides are silica (59.26%), alumina (10.39%), and calcite (10.42%), which gives it a sandy loam character according to the geotechnical classification. Finally, GBFS has silica, calcium, and alumina oxide percentages of 38%, 42.9%, and 10.8%, respectively. The physical properties of the sediment, FA, and GBFS are summarized in Table 2. The specific gravity of FA and GBFS were 2.20 and 2.91 g/cm^3, respectively, and Blaine Fineness was 3100 and 4450 cm^2/g, respectively.

Table 2. Raw material chemical and mineralogical compositions.

Materials	LOI	CaO	SiO_2	Al_2O_3	Fe_2O_3	MgO	SO_3	Na_2O	K_2O
S	5.95	10.42	59.26	10.39	3.34	1.33	0.5	0.67	1.93
FA	4.19	2.66	50.49	25.32	7.58	1.33	0.75	0.54	3.73
GBFS	<1.5	42.9	38.0	10.8	0.7	6.6	0.1	0.28	0.35

The alkaline solution of sodium hydroxide (NaOH) is the most used activating element in the formulation of geopolymers. It reacts perfectly with fly ash and GBFS precursors. Its low cost and low viscosity make it the best known and sold on the market. In addition, the leaching of Al_3^+ and Si_4^+ ions are practically high with NaOH solution compared to potassium hydroxide (KOH) solution [30]. Dissolving NaOH in water releases hydroxide anions (OH^-) that act as a catalyst for the dissolution of aluminosilicate contains the precursor (FA and GBFS) in the first step and the sodium cation (Na^+), which participates as a structuring element and balances the charge of the geopolymers in order to insure the stability of the matrix [31]. NaOH has significantly affected the compressive strength and the structure of geopolymers [31]. In this study, an 8M sodium hydroxide solution was adopted for all mixtures.

The particle size distribution graph is presented in Figure 6 and Tables 3 and 4. The sample of raw sediments contains sand (62.39%), silt (33.91%), and clay (3.69%), which gave it the silty sand character. The grain size curve was not entirely within the grain size zone, which is recommended by the CRATerre-EAG standard [21]. However, the clay part is generally accepted even though it falls outside the recommended areas since it can still give acceptable results in practice. On the other hand, soils which do conform will, in most cases, give good results. The shaded areas are guidelines for the user and not specifications to be rigidly applied [21]. However, in the manufacture of traditional compressed earth stabilized by lime or clinker cement, the clayey part must be respected because of its main role in the reaction for the hardening of the product. Moreover, in the case of compressed earth blocks based on geopolymers binder, the precursor powders are responsible for the hardening and the mechanical resistance of the blocks.

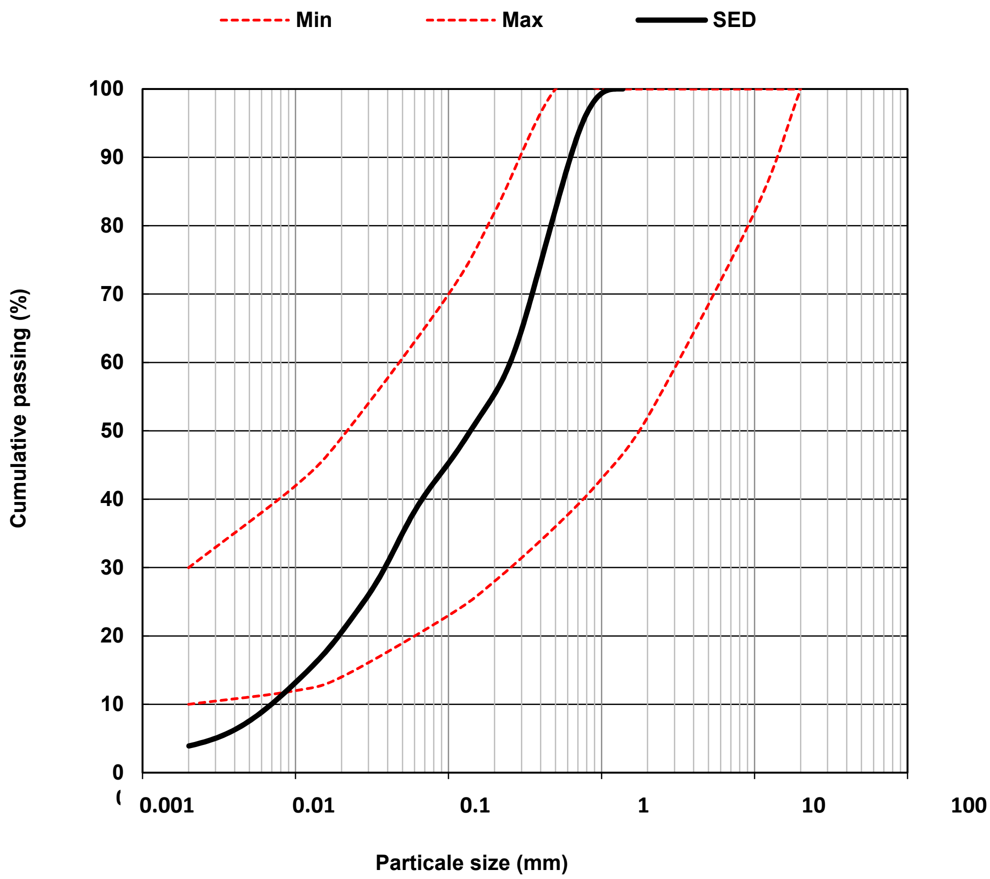

Figure 6. Raw sediments particle size distribution.

Table 3. Sediment physical properties.

Element	Size Distribution of Sediment (%)
Sand	62.39
Silt	33.91
Clay	3.91

Table 4. Raw material physical properties.

Materials	Specific Gravity (g/cm^3)	Methylene Blue Value (g/100 g)
S	2.59	2
FA	2.20	/
GBFS	2.90	/

The compressed sediment block mixes are summarized in Table 5. The first four mixes (F1 to F4) contain only sediment and fly ash. The percentage of fly ash increases by about 10% while the percentage of sediment decreases by about 10%. On the other hand, a percentage of 10% of GBFS are added to the last four formulations (F1′ to F4′) while adjusting the percentage of sediment and fly ash.

Table 5. Percentage of basic materials for each type of CEB.

Mix	Source Materials	S (%)	FA (%)	GBFS (%)	NH (%)
F1	S + FA	90	10	0	18.24
F2	S + FA	80	20	0	18.64
F3	S + FA	70	30	0	19.30
F4	S + FA	60	40	0	20.77
F1′	S + FA + GBFS	81	9	10	20.24
F2′	S + FA + GBFS	72	18	10	20.64
F3′	S + FA + GBFS	63	27	10	21.30
F4′	S + FA + GBFS	54	36	10	22.77

3.2. CEB Physical and Mechanical Properties

3.2.1. Compressive Strength

The results of the 14- and 28-day compression strengths of the CEB samples are shown in Figure 7. The sample compressive strengths have obviously increased with the increase in the percentage of FA. For the first four mixes, the 14th day compressive strengths for the mixes F1, F2, F3, and F4 were equal to 4.56, 5.07, 7.16, and 9.07 MPa, respectively. However, the 28th day compressive strengths slightly decreased. This decrease may be caused by micro-cracks, which may be created during the block maturation. The mixes using FA and GBFS exhibited very high 28th day strengths. The 28th day compressive strength of mix F4′, which reached the value of 16.53 MPa, has exceeded the value of 4 MPa recommended by the standard XP P13- 901 for compressed earth blocks. However, the compressive strengths of all mixes were very satisfactory. The compressive strengths of few mixes were almost four times those needed to withstand higher loads. Furthermore, the obtained compressive strengths are more competitive with other previous studies, such as S. Larbi and J. Rivera with 6.64 MPa [32] and 12 MPa [5], respectively.

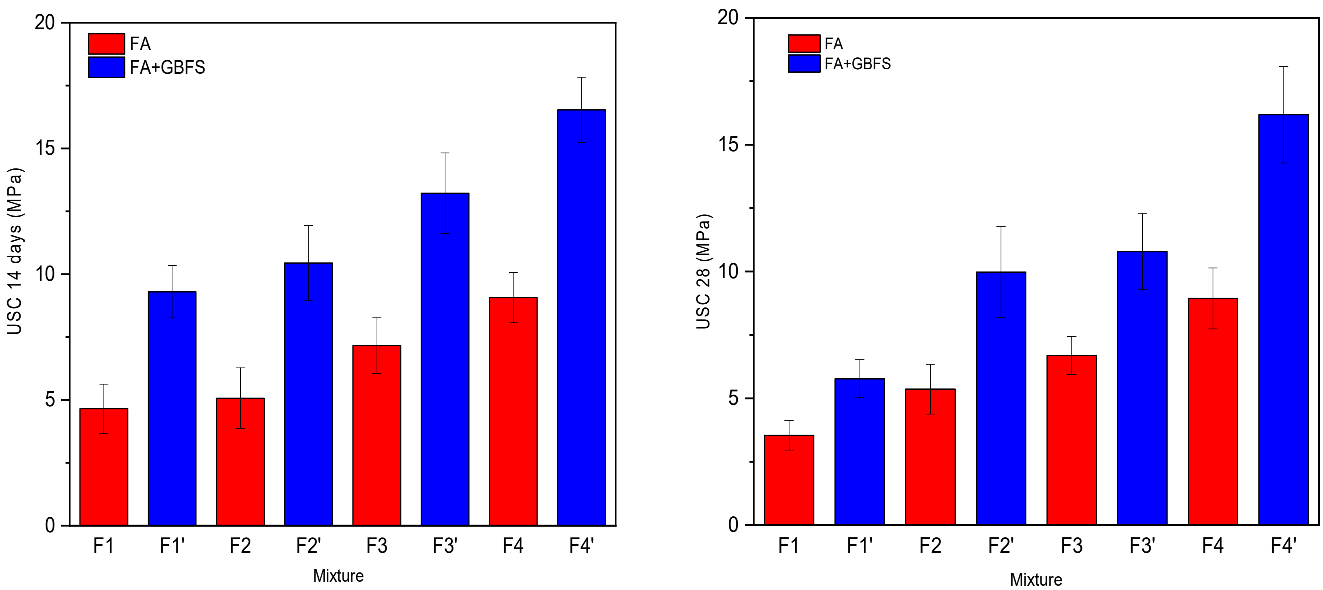

Figure 7. Compressive strengths at 14 and 28 days for different mixtures.

However, the compression strengths of mixes with FA and GBFS are almost double those of FA mixes. The available free calcium ions (Ca^{++}), which reacted with silica and alumina, formed more hydrated calcium alumina silicate gel (CASH) that coexisted with geopolymers gels [20,33]. Moreover, a portlandite formation occurs when the lime containing GBFS gets in contact with the water present in the mix. On the other hand, the GBFS reacts with alkaline solutions in an exothermic process that generates more heat for a good geo-polymerization reaction. The reaction between the sodium hydroxide solution and aluminosilicate containing fly ash and blast furnace slag leads to the release of a large quantity of [$SiO(OH)_3$] and [$Al(OH)_4$]. This in turn allows the formation of geopolymer gels consisting of a large three-dimensional array of aluminosilicate responsible for the hardening of the mix.

3.2.2. Dynamic Young's Modulus

The 28th day dynamic Young's modulus values of CEBs, which are summarized in Figure 8, had a similar trend as compressive strengths. The maximum values of dynamic young modulus were obtained for F4′ based FA + GBFS (10.3 GPa); this value confirms the optimum recorded mechanical resistance of 16.53 MPa

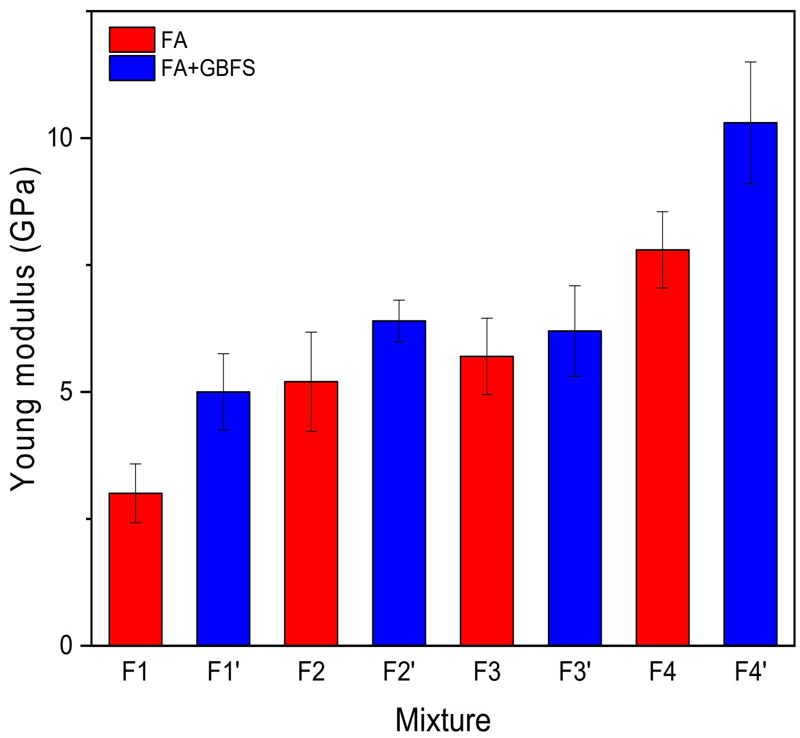

Figure 8. Dynamic Young's modulus of different mixtures.

3.2.3. Water Sensitivity of Compressed Sediment Block Samples

Figure 9 shows the water sensitivity of compressed sediment block samples. However, all the mixes based on fly ash (F1, F2, F3, and F4) have dark watercolor and some disaggregation in the bottom of the glass container. This is explained by the material dissolution in the presence of water and probably due to the release of very fine sediment particles and insufficiency of alkaline activator for producing more gels. Otherwise, mixes that are based FA and GBFS have less dark color. Moreover, the mix F4′ with (54% S 34% FA 10% GBFS), whose watercolor is relatively clear, is the only one thart is admissible. In fact, the test is essential for simulating the water damage that is generally caused by rainwater attacks.

3.2.4. Capillarity of Compressed Block's

Figure 10 shows the water absorption by capillarity of CEBs after 28 days. This characteristic has not been considered for the block intended for use in dry medium. However, the sample F1′ (81S 09FA 10GBFS) had the highest capillarity absorption value. The remaining mixes with or without GBFS do not violate the capillarity limit threshold (Cb), which is lower than 20 $g/cm^2 \cdot min^{0.5}$ (dotted line in Figure 10). Furthermore, the best value is the one recorded for the mix F4′ (54S 36FA 10GBFS), for which the Cb was around 6 units. Therefore, the absorption results were in accordance with the mechanical ones.

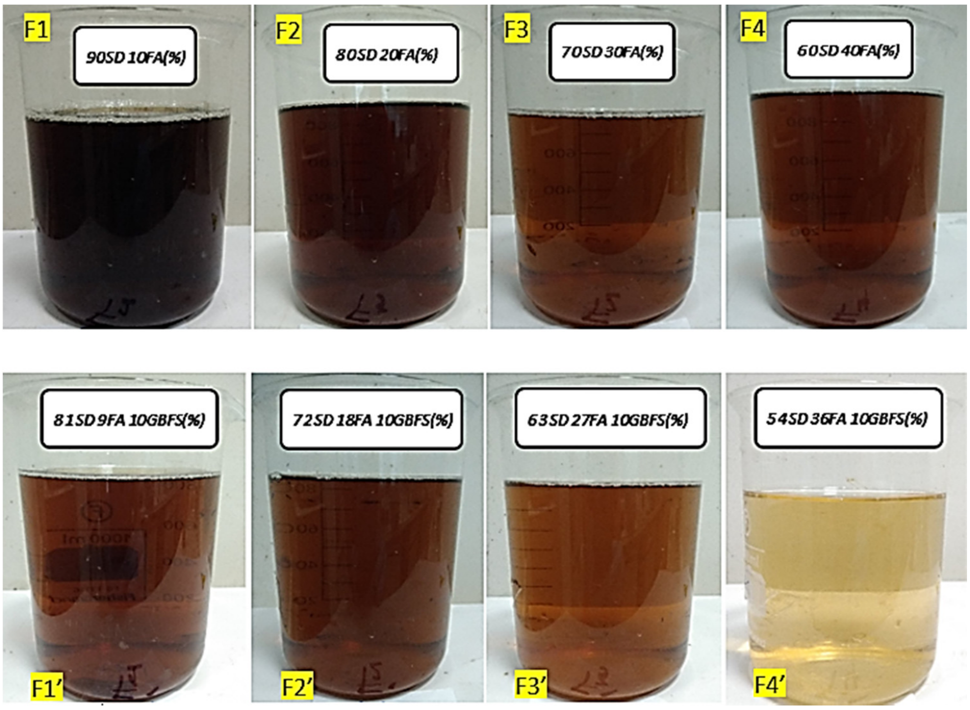

Figure 9. Sample water sensitivity.

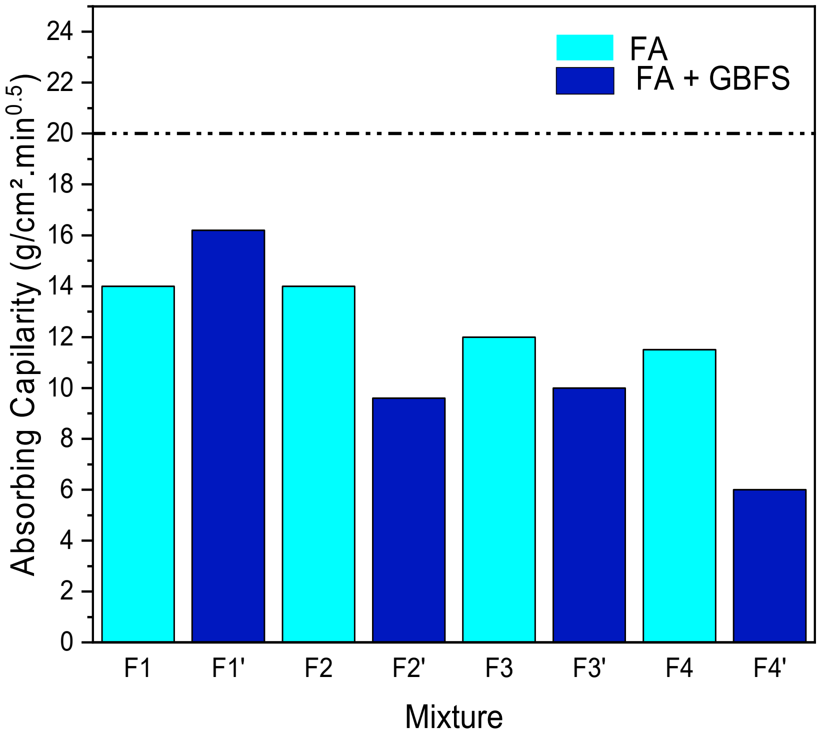

Figure 10. CEB water absorption coefficient after 28 days of cure.

Figure 11 shows the correlations between the compressive strengths, the Young's modulus, and the water absorption of the various formulations. It appears that the compressive strength is proportional to the Young's modulus. On the other hand, the compressive strengths are inversely proportional to the absorption of water. These results can be related to the compactness of the mixtures, which is also proportional to the mechanical strength and the porosity.

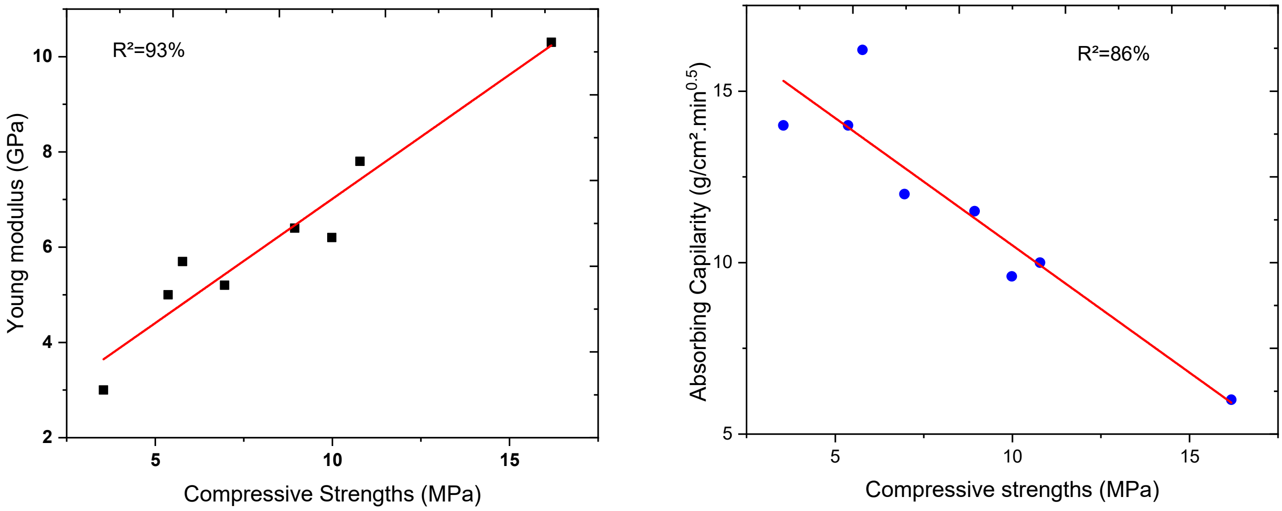

Figure 11. Correlation between mechanical strength, Young's Modulus, and absorption capacity.

3.2.5. Microstructure Observations

The results of scanning electron microscope of the fractured surface of geopolymer mixes F4 and F4′ (54S 36FA 10GBFS) are shown in Figure 12. Overall, the mix F4′ shows a dense form of gels, more than that of F4. This dense mass can be practically associated with NASH and some of Hydrosodalite (Figure 12f). The mixes based on FA also had more gels than CASH and CSH. This has been confirmed by the high compression strength results (up to 16.18 MPa in Figure 7). However, the micrograph showed the spherical particles of fly ash with their initial spherical shape (Figure 12e), which indicates the non-reaction with alkaline solution while the shell form (Figure 12d) presents the particles of fly ash that are not completely consumed by sodium hydroxide solution.

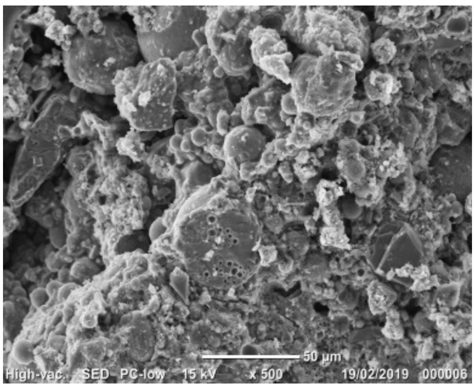

(**a**)

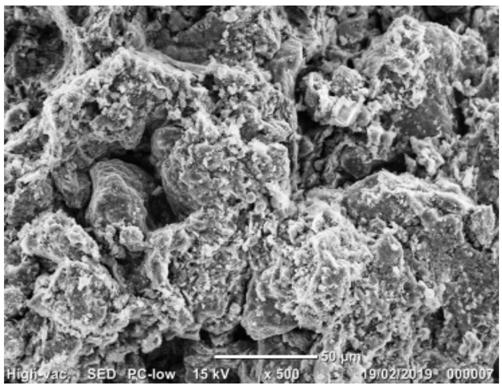

(**b**)

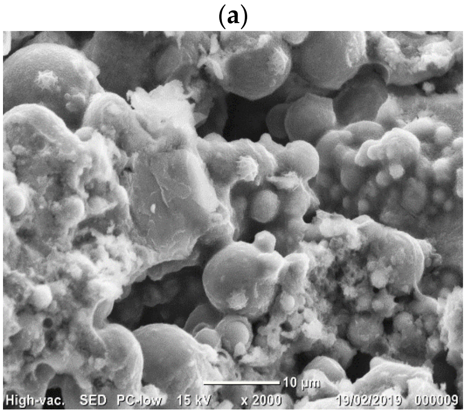

(**c**)

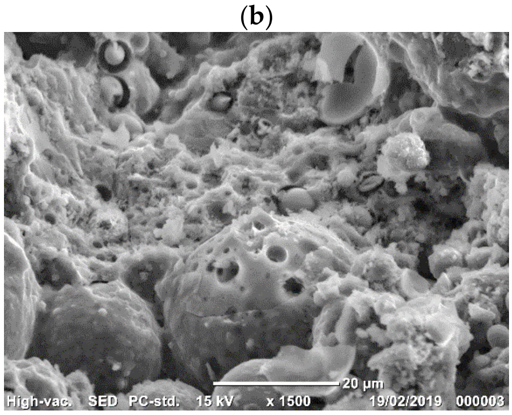

(**d**)

Figure 12. *Cont.*

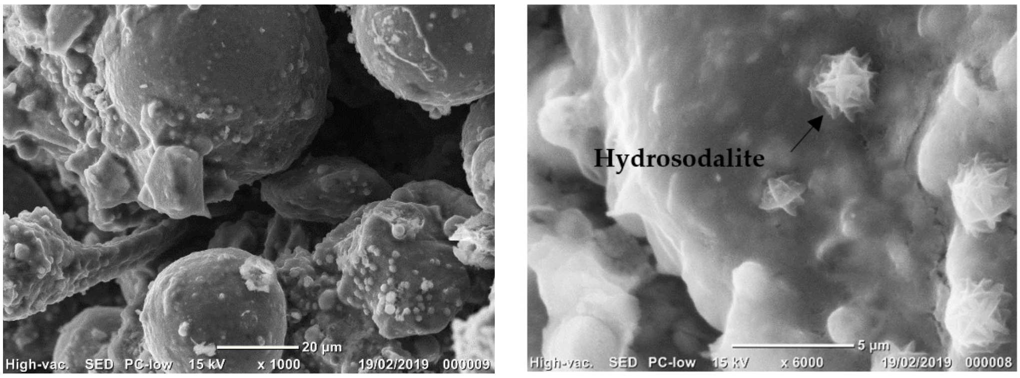

(**e**) (**f**)

Figure 12. Scanning Electron Microscopy observations of CEB ((**a**,**c**,**e**) for F4 and (**b**,**d**,**f**) for F4′).

3.2.6. Infrared Red Spectroscopy Analysis

The samples were analyzed using the KBr tablet method: putting both compressed block powder with a transparent alkali halide KBr, using for this an agate mortar for grinding, adding the product in the sample holder, and compressing hard to perfectly obtain the sample.

Figure 13 shows the transmission mode of FTIR spectra for F4′ mix using the conventional wave numbers for molecular vibration of different bonds. The spectral range that was used to characterize this type of material was between 600 and 4000 cm^{-1}. The small bands are located between 600 and 800 cm^{-1}, which are attributed to the bonds present in the fly ash source (quartz and mullite) [34]. The band was 1030 cm^{-1} with asymmetric Al–O/Si–O stretching [35]. The appearance of a band at 1430 cm^{-1} may be due to C=O vibrations, confirming the presence of carbonate groups [36]. Two more bands were located. The first band was between 1600 and 1650 cm^{-1} while the second was around 3450 cm^{-1}. However, since these bands are generated by water molecules, they are indicators of the hydration of the geopolymer material [15].

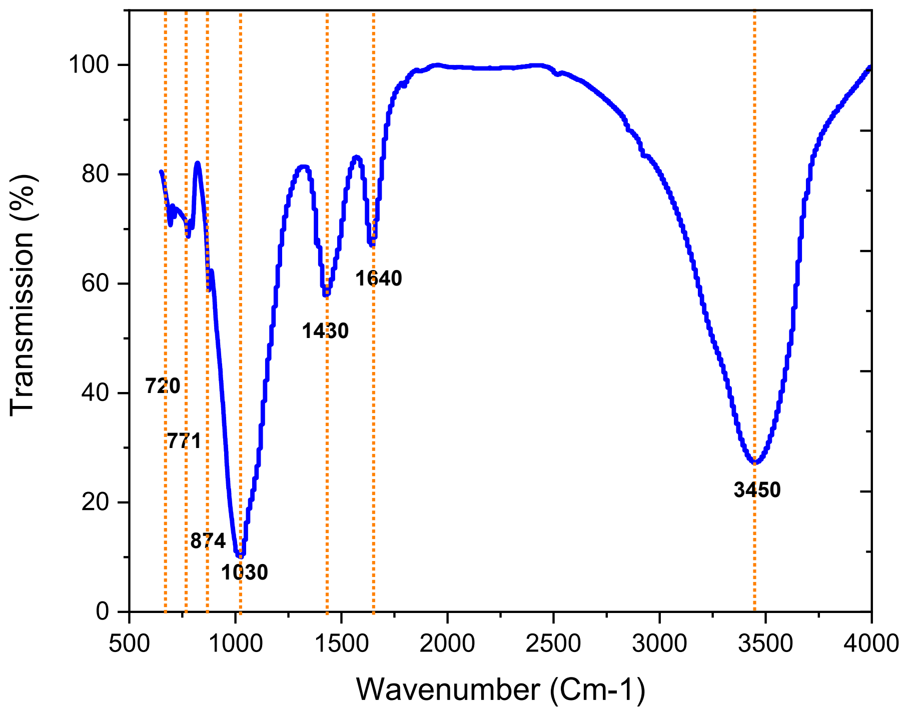

Figure 13. F4′ (FA + GBFS mix) FTIR spectra.

4. Conclusions

The purpose of the study was to valorize dredged sediments from northern France as a sand for the manufacture of new compressed blocks that are cheaper and more environmentally friendly than the traditional ones prepared with clinker cement. The study highlights the possibility of manufacturing compressed blocks using an ecological geopolymer binder that emits less CO_2. It would be important to focus a future study on a life cycle assessment (LCA) and the hydrothermal behavior of these new solutions.

The specific objectives of the study were to evaluate the physical, mechanical, and microstructure properties of this new product. The following conclusions can be drawn from the study:

1. All mixes had higher mechanical strengths than recommended by the standard.
2. The obtained highest compressive strength of more than 16.18 MPa represents an optimal value for the compressed earth blocks.
3. Water sensitivity is a major parameter because blocks are frequently exposed to rainwater. The sample F1′ had the highest capillarity absorption value. The remaining mixes with or without GBFS did not violate the capillarity limit threshold, which is lower than 40.
4. The combination of fly ash and slag with well-studied percentages can give impressive results around 16.18 MPa against 8.94 MPa without GBFS
5. The gels molecules produced by geopolymer binders have more efficiency than that of traditional CEB communicated by the obtained mechanical strengths of previous work found in the literature.

Author Contributions: Conceptualization, F.B. and W.M.; Data curation, F.B., W.M. and M.B.; Formal analysis, N.-E.A.; Investigation, F.B.; Project administration, M.B. and N.-E.A.; Resources, W.M. and N.-E.A.; Validation, W.M.; Visualization, W.M. and A.S.; Writing—original draft, F.B.; Writing—review & editing, W.M. All authors have read and agreed to the published version of the manuscript.

Funding: This research received no external funding.

Institutional Review Board Statement: Not applicable.

Informed Consent Statement: Not applicable.

Data Availability Statement: Not applicable.

Conflicts of Interest: The authors declare no conflict of interest.

References

1. Pierrehumbert, R. There is no Plan B for dealing with the climate crisis. *Bull. At. Sci.* **2019**, *75*, 215–221. [CrossRef]
2. Bellara, S.; Hidjeb, M.; Maherzi, W.; Mezazigh, S.; Senouci, A. Optimization of an Eco-Friendly Hydraulic Road Binders Comprising Clayey Dam Sediments and Ground Granulated Blast-Furnace Slag. *J. Build.* **2021**, *11*, 443. [CrossRef]
3. Apitz, S.E. Waste or resource? Classifying and scoring dredged material management strategies in terms of the waste hierarchy. *J. Soils Sediments* **2010**, *10*, 1657–1668. [CrossRef]
4. Morel, J.-C.; Mesbah, A.; Oggero, M.; Walker, P. Building houses with local materials: Means to drastically reduce the environmental impact of construction. *Build. Environ.* **2001**, *36*, 1119–1126. [CrossRef]
5. Rivera, J.; Coelho, J.; Silva, R.; Miranda, T.; Castro, F.; Cristelo, N. Compressed earth blocks stabilized with glass waste and fly ash activated with a recycled alkaline cleaning solution. *J. Clean. Prod.* **2021**, *284*, 124783. [CrossRef]
6. Pacheco-Torgal, F.; Jalali, S. Earth construction: Lessons from the past for future eco-efficient construction. *Constr. Build. Mater.* **2012**, *29*, 512–519. [CrossRef]
7. Kumar, S.; Kumar, R.; Mehrotra, S.P. Influence of granulated blast furnace slag on the reaction, structure and properties of fly ash based geopolymer. *J. Mater. Sci.* **2010**, *45*, 607–615. [CrossRef]
8. Bagheri, A.; Nazari, A. Compressive strength of high strength class C fly ash based geopolymers with reactive granulated blast furnace slag aggregates designed by Taguchi method. *Mater. Des.* **2014**, *54*, 483–490. [CrossRef]
9. Diaz, E.I.; Allouche, E.N.; Eklund, S. Factors affecting the suitability of fly ash as source material for geopolymers. *Fuel* **2010**, *89*, 992–996. [CrossRef]
10. Phoo-ngernkham, T.; Chindaprasirt, P.; Sata, V.; Pangdaeng, S.; Sinsiri, T. Properties of high calcium fly ash geopolymer pastes containing Portland cement as additive. *Int. J. Miner. Metall. Mater.* **2013**, *20*, 214–220. [CrossRef]

11. Phoo-ngernkham, T.; Chindaprasirt, P.; Sata, V.; Sinsiri, T. High calcium fly ash geopolymer containing diatomite as additive. *Indian J. Eng. Mater. Sci.* **2013**, *20*, 310–318.
12. Palomo, A.; Fernandez-Jimenez, A.; Kovalchuk, G.; Ordonez, L.M.; Naranjo, M.C. Opc-fly ash cementitious systems: Study of gel binders produced during alkaline hydration. *J. Mater. Sci.* **2007**, *42*, 2958–2966. [CrossRef]
13. Williams, P.J.; Biernacki, J.J.; Walker, L.R.; Meyer, H.M.; Rawn, C.J.; Bai, J. Microanalysis of alkali-activated fly ash–CH pastes. *Cem. Concr. Res.* **2002**, *32*, 963–972. [CrossRef]
14. Ravikumar, D.; Peethamparan, S.; Neithalath, N. Structure and strength of NaOH activated concretes containing fly ash or GGBFS as the sole binder. *Cem. Concr. Compos.* **2010**, *32*, 399–410. [CrossRef]
15. Somna, K.; Jaturapitakkul, C.; Kajitvichyanukul, P.; Chindaprasirt, P. NaOH activated ground fly ash geopolymer cured at ambient temperature. *Fuel* **2011**, *90*, 2118–2124. [CrossRef]
16. Guo, X.; Shi, H.; Chen, L.; Dick, W.A. Alkali-activated complex binders from class C fly ash and Ca-containing admixtures. *J. Hazard. Mater.* **2010**, *173*, 480–486. [CrossRef]
17. Aydın, S.; Baradan, B. Effect of activator type and content on properties of alkali activated slag mortars. *Compos. B Eng.* **2014**, *57*, 166–172. [CrossRef]
18. Puertas, F.; Martinez-Ramirez, S.; Alonso, S.; Vazquez, T. Alkali-activated fly ash/slag cements: Strength behavior and hydration products. *Cem. Concr. Res.* **2000**, *30*, 1625–1632. [CrossRef]
19. Ismail, I.; Bernal, S.A.; Provis, J.L.; San Nicolas, R.; Hamdan, S.; van Deventer, J.S.J. Modification of phase evolution in alkali-activated blast furnace slag by the incorporation of fly ash. *Cem. Concr. Compos.* **2014**, *45*, 125–135. [CrossRef]
20. Garcia-Lodeiro, I.; Fernandez-Jimenez, A.; Palomo, A. Hydration kinetics in hybrid binders: Early reaction stages. *Cem. Concr. Compos.* **2013**, *39*, 82–92. [CrossRef]
21. CRATerre; Houben, H.; Boubekeur, S. Blocs de Terre Comprimée: Normes. Guide CDE, Série Technologie n°11, CRATerre-EAG, Villefontaine/Bruxelles, France/Belgique, 142p. 1998. Available online: https://craterre.hypotheses.org/files/2017/05/7502_BTC_Normes.pdf (accessed on 6 February 2022).
22. *NF P94-093*; Standard Détermination des Références de Compactage d'un Matériau—Proctor Normal et Proctor Modifié. 1999. Available online: https://pdfslide.net/documents/nf-p-94-093-proctor-99.html (accessed on 6 February 2022).
23. *NF P 94-100*; Standard Soils: Reconnaissance and Tests—Materials Treated with Lime and/or Hydraulic Binders—Tests to Assess the Suitability of a Soil for Treatment. Available online: https://www.boutique.afnor.org/en-gb/standard/nf-p94100/soils-investigation-and-testing-lime-and-or-hydraulic-binder-treated-materi/fa059725/45687 (accessed on 6 February 2022).
24. *X11-667*; Standard Particle Size Analysis Laser Optical mEthod Mesasurment of Trasition Period. Available online: https://arenatecnica.com/en/technical-standards/bs_iso_20998-2#last-publication-date (accessed on 6 February 2022).
25. *NF P94-068*; Standard Measurement of the Methylene Blue Adsorption Capacity of a Soil or a Rocky Material—Determination of the Methylene Blue Value of a Soil or a Rocky Material by the Spot Test. Available online: https://www.boutique.afnor.org/en-gb/standard/nf-p94068/soils-investigation-and-testing-measuring-of-the-methylene-blue-adsorption-/fa043689/394 (accessed on 6 February 2022).
26. *NF EN 1097-7*; Standard Tests to Determine the Mechanical and Physical Characteristics of Aggregates—Part 7: Determination of the Absolute Density of Filler—Pycnometer Method. Available online: https://standards.iteh.ai/catalog/standards/cen/f8079242-62c6-45aa-b978-cc250d8a9222/en-1097-7-2008 (accessed on 6 February 2022).
27. Omar Sore, S.; Messan, A.; Prud'homme, E.; Escadeillas, G.; Tsobnang, F. Stabilization of compressed earth blocks (CEBs) by geopolymer binder based on local materials from Burkina Faso. *Constr. Build. Mater.* **2018**, *165*, 333–345. [CrossRef]
28. *NF EN 196-1*; Standard Methods of Testing Cement—Part 1: Determination of Strength. Available online: https://standards.iteh.ai/catalog/standards/cen/37b8816e-4085-4dcc-a642-a383d9bddd6c/en-196-1-2016 (accessed on 6 February 2022).
29. *XP P 13-901*; Standard Compressed Earth Blocks for Walls and Partitions—Definitions—Specifications—Test methods—Delivery Acceptance Conditions. Available online: https://standards.globalspec.com/std/811579/XP%20P13-901 (accessed on 6 February 2022).
30. Van Jaarsveld, J.G.S.; van Deventer, J.S.J. Effect of the alkali metal activator on the properties of fly ash-based geopolymer. *Ind. Eng. Chem. Res.* **1999**, *38*, 32–41. [CrossRef]
31. Gohan, G.; Kurklu, G. The Influence of NaOH solution on the properties of Fly Ash based geopolymer Mortar cured at Different Temperature. *Compos. Part B* **2014**, *58*, 371–377. [CrossRef]
32. Larbi, S.; Khaldi, A.; Maherzi, W.; Abriak, N.E. Formulation of compressed earth blocks stabilized by glass waste activated with naoh solution. *Sustainability* **2022**, *14*, 102. [CrossRef]
33. Divet, L.; Le Roy, R.; Van Rompaey, G. *Hydratation des Laitiers de Haut Fourneau, Rapport LCPC*; LCPC, ENPC, HOLCIM Paris: Marne la Vallée, Belgique, 2006.
34. Casarez, R. Experimental study of XRD, FTIR and TGA techniques in geopolymeric materials. *Int. J. Adv. Comput. Sci. Appl.* **2014**, *4*, 221–226. [CrossRef]
35. Kumar, S.; Kumar, R. Mechanical activation of fly ash: Effect on reaction, structure and properties of resulting geopolymer. *J. Mater. Sci.* **2011**, *45*, 607–615. [CrossRef]
36. Singh, N. Fly Ash-Based Geopolymer Binder: A Future Construction Material. *Minerals* **2018**, *8*, 299. [CrossRef]